Author(s): Konu, Jari; Chivers, Tristram; Tuononen, Heikki

Title: Synthesis, Spectroscopic, and Structural Investigation of the Cyclic [N(PR2E)2]+ Cations (E = Se, Te; R = iPr, Ph): the Effect of Anion and R-Group Exchange

Year: 2006

Version:

Please cite the original version:

Konu, J., Chivers, T., & Tuononen, H. (2006). Synthesis, Spectroscopic, and Structural Investigation of the Cyclic [N(PR2E)2]+ Cations (E = Se, Te; R = iPr, Ph): the Effect of Anion and R-Group Exchange. Inorganic Chemistry, 45(26), 10678-10687. https://doi.org/10.1021/ic061545i

Synthesis, Spectroscopic and Structural Investigation of the Cyclic $[N(PR_2E)_2]^+$ Cations (E = Se, Te; R = ^{i}Pr, Ph): The Effect of Anion and R-group Exchange

Jari Konu,[†] Tristram Chivers,*[†] and Heikki M. Tuononen[‡]

Department of Chemistry, University of Calgary, 2500 University Drive N.W., Calgary, Alberta, Canada T2N 1N4, and Department of Chemistry, University of Jyväskylä, P.O. Box 35, Jyväskylä, FI-40014, Finland.

E-mail: chivers@ucalgary.ca

Tel: +1-403-220-5741

Fax: +1-403-289-9488

† University of Calgary

‡ University of Jyväskylä

Abstract

Two-electron oxidation of the $[N(P^iPr_2E)_2]^-$ anion with iodine produces the cyclic $[N(P^iPr_2E)_2]^+$ (E = Se, Te) cations, which exhibit long E-E bonds in the iodide salts $[N(P^iPr_2Se)_2]I$ (**4**) and $[N(P^iPr_2Te)_2]I$ (**5**). The iodide salts **4** and **5** are converted to the ion-separated salts $[N(P^iPr_2Se)_2]SbF_6$ (**6**) and $[N(P^iPr_2Te)_2]SbF_6$ (**7**) upon treatment with $AgSbF_6$. The compounds **4**-**7** were characterized in solution by multinuclear NMR, vibrational and UV-visible spectroscopy supported by DFT calculations. A structural comparison of the salts **4**, **5**, **6**, **7** and $[N(P^iPr_2Te)_2]Cl$ (**8**) confirms that the long E-E bonds in **4, 5** and **8** can be attributed primarily to the donation of electron density from lone pair of the halide counter-ion into the E-E σ* orbital (LUMO) of the cation. The phenyl derivative $[N(PPh_2Te)_2]I$ (**9**) was prepared in a similar manner. However, the attempted synthesis of the selenium analog, $[N(PPh_2Se)_2]I$, produced a 1:1 mixture of $[N(PPh_2Se)_2(\mu\text{-}Se)][I]$ (**10**) and $[SeP(Ph_2)N(Ph_2)PI]$ (**11**). DFT calculations of the formation energies of **10** and **11** support the observed decomposition. Compound **10** is a centrosymmetric dimer in which two six-membered NP_2Se_3 rings are bridged by two I^- anions. Compound **11** produces the nine-atom chain $\{[N(PPh_2)_2Se]_2(\mu\text{-}O)\}$ (**12**) upon hydrolysis during crystallization. The reaction between $[(TMEDA)NaN(P^iPr_2Se)_2]$ and $SeCl_2$ in a 1:1 molar ratio yields the related acyclic species $[SeP(^iPr_2)N(^iPr_2)PCl]$ (**13**), which was characterized by multinuclear NMR spectroscopy and an X-ray structural determination.

Introduction

Dichalcogenoimidodiphosphinate ligands $[N(PR_2E)_2]^-$ **1** (E = O, S, Se) have a long and venerable history that dates back to the 1960s.[1] The widespread interest in their metal complexes[2] arises from a number of potential uses *e.g.,* as lanthanide shift reagents,[3] in luminescent materials,[4] or in metal extraction processes.[5] Recently, O'Brien and co-workers have demonstrated that certain complexes of the isopropyl derivatives **1a** and **1b** are sufficiently volatile to serve as single-source precursors for the production of thin semi-conducting films of metal selenides.[6]

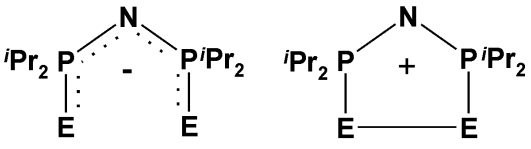

1a (E = S)
1b (E = Se)
1c (E = Te)

3a (E = S)
3b (E = Se)
3c (E = Te)

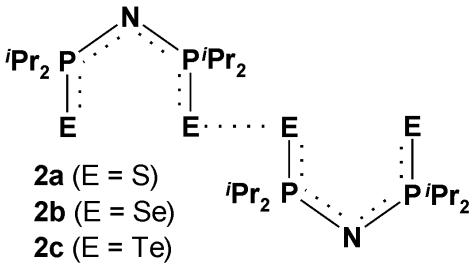

2a (E = S)
2b (E = Se)
2c (E = Te)

The neutral precursors to the anionic ligands **1a** and **1b** are readily made by direct reaction of $HN(P^iPr_2)_2$ with elemental sulfur or selenium, respectively,[7] but this reaction is not successful for the synthesis of $HN(P^iPr_2Te)_2$. Four years ago we reported the synthesis of the tellurium-containing ligands $[N(PR_2Te)_2]^-$ (R = ^{i}Pr, Ph) by metallation of $HN(PR_2)_2$ with NaH *prior to reaction with tellurium*.[8, 9] The discovery of this new synthetic approach has opened the door to a wide-ranging study of metal complexes of **1c**. To date, homoleptic complexes of Group 12 (Zn, Cd, Hg) and Group 15 (Sb, Bi),[10] as well as a La(III) complex and the first example of a covalent actinide-tellurium bond have been reported.[11] Some of these complexes have been shown to be suitable single-source precursors for metal telluride thin films or nanoparticles, *e.g.*

CdTe,[12] Sb_2Te_3.[13] In contrast to the metathetical reactions observed for Groups 12 and 15 halides, the treatment of **1c** with Group 13 (Ga, In) trihalides gives rise to a novel tellurium-transfer process and the formation of Ga_2Te_2 and In_3Te_3 rings.[14]

An intriguing feature of the chemistry of **1c** is the formation of unusual dichalcogenides of the type **2** upon one-electron oxidation of the sodium salts with iodine. [9, 15] This redox process represents a new aspect of the well-studied chemistry of dichalcogenoimidodiphosphinates and raised the fascinating question of whether the corresponding cations **3b** and **3c** can be prepared by two-electron oxidation of the corresponding anions **1b** or **1c** (or one-electron oxidation of the dimers **2b** and **2c**). In a preliminary communication,[16] we described the synthesis of the iodide salts $[N(P^iPr_2Se)_2]I$ (**4**) and $[N(P^iPr_2Te)_2]I$ (**5**), which contain the cyclic cations **3b** and **3c**, respectively. Simple electron-counting procedures for these novel inorganic heterocycles predict a six π-electron system.[17] However, DFT calculations revealed that, although the three highest occupied molecular orbitals in the five-membered rings **3** are π-type orbitals, the bonding effect of the E-E π-bonding orbital (HOMO-2) is essentially cancelled by the double occupation of the E-E π*-antibonding orbital (HOMO). Since the third π orbital (HOMO-1) is a non-bonding orbital located primarily on the nitrogen atom, the π-bond order of the ring system is approximately zero.

DFT calculations also indicated that the unusually long chalcogen-chalcogen bonds observed in the iodide salts **4** and **5** may be attributed primarily to donation of electron density from a lone pair of the iodide counter-ion into the E-E σ* orbital (LUMO) of the cyclic cation.[16] We have now extended the investigation of this new five-membered ring system to include ion-separated salts in order to gain experimental verification for this explanation. In addition, the effect of the replacement of the isopropyl substituents on phosphorus by phenyl groups was examined. Thus, we report herein the synthesis, spectroscopic and structural characterization of the following salts of these five-membered rings $[N(P^iPr_2Se)_2]SbF_6$ (**6**), $[N(P^iPr_2Te)_2]SbF_6$ (**7**), $[N(P^iPr_2Te)_2]Cl$ (**8**) and $[N(PPh_2Te)_2]I$ (**9**). The unexpected formation of the six-membered ring

$[N(PPh_2Se)_2(\mu\text{-}Se)][I]$ (**10**) and the acyclic species $[SeP(Ph_2)N(Ph_2)PI]$ (**11**) in the attempted synthesis of $[N(PPh_2Se)_2]I$ is also described together with the X-ray structure of the nine-atom chain $\{[N(PPh_2)_2Se]_2(\mu\text{-}O)\}\bullet CH_2Cl_2$ (**12**$\bullet CH_2Cl_2$). The synthesis and X-ray structure of the acyclic compound $[SeP(^iPr_2)N(^iPr_2)PCl]$ (**13**), an analogue of **11**, are also discussed.

Experimental Section

General Procedures. All reactions and manipulations of products were performed under an argon atmosphere by using standard Schlenk techniques or an inert atmosphere glove box. $[N(P^iPr_2E)_2]I$ (**4**, E = Se; **5**, E = Te) were prepared by the method described recently.[16] The complete spectroscopic data (^1H, ^{13}C, ^{31}P, ^{77}Se, ^{125}Te NMR, IR and Raman, UV-visible) and relevant bond parameters for **4** and **5** are included here for comparison with those of **6** and **7**. The reagents $[(TMEDA)NaN(PR_2E)_2]$ (E = Se, Te; R = ^{i}Pr, Ph) were prepared by modifications of the procedure reported for $[(TMEDA)NaN(PPh_2Te)_2]$.[8] $SeCl_2$ was prepared from red selenium and SO_2Cl_2 in THF.[18] The solvents n-hexane, toluene and THF were dried by distillation over Na/benzophenone and CH_2Cl_2 over P_2O_5 under a nitrogen atmosphere prior to use.

Spectroscopic Methods. The ^1H, ^{13}C, ^{31}P, ^{77}Se and ^{125}Te NMR spectra were obtained in d_8-THF or CD_2Cl_2 on a Bruker DRX 400 spectrometer operating at 399.592, 100.489, 161.765, 76.223 and 126.082 MHz, respectively. ^1H and ^{13}C spectra are referenced to the solvent signal and the chemical shifts are reported relative to $(CH_3)_4Si$. ^{31}P and ^{77}Se NMR spectra are referenced externally to an 85% solution of H_3PO_4 and to a saturated solution of SeO_2 in D_2O, respectively, and the chemical shifts are reported relative to H_3PO_4 and to neat Me_2Se [$\delta(Me_2Se) = \delta(SeO_2) + 1302.6$]. The ^{125}Te NMR spectra are referenced externally to a saturated solution of H_6TeO_6 and the ^{125}Te chemical shifts are reported relative to Me_2Te [$\delta(Me_2Te) = \delta(H_6TeO_6) + 712$].

Raman spectra were recorded at the University of Lethbridge from solid samples at -100 °C by using a Bruker RFS 100 FT-Raman spectrometer with a quartz beam splitter, liquid-nitrogen-cooled Ge detector and Nd:YAG laser (power 25-100 mW; 500-1000 scans; spectral resolution ±2 to ±8 cm^{-1}; Blackmann-Harris four-term apodization; scattering geometry 180 °). IR spectra were measured as Nujol mulls between KBr plates on a Mattson Genesis Series FT-IR (4000-400 cm^{-1}) spectrometer. A list of IR-and Raman vibrations can be found in the Supplementary Information (Table S1). Elemental analyses were performed by Analytical Services, Department of Chemistry, University of Calgary. UV-Visible spectra were measured with a Cary 50 spectrophotometer (200-800 nm, scan rate 600 nm/min, dual beam) in CH_2Cl_2 and MeCN.

Spectroscopic data of [N(P^{i}Pr$_2$Se)$_2$]I (4).[16] ^{1}H NMR (D_8-THF, 23 °C): δ = 2.73 [2 x sept., $^3J(^1H,^1H)$ = 7 Hz, 4H; C*H*(CH_3)$_2$], 1.37 [dd, $^3J(^1H,^1H)$ = 7 Hz, $^3J(^1H,^{31}P)$ = 18 Hz, 12H; CH(C*H*$_3$)$_2$], 1.35 [dd, $^3J(^1H,^1H)$ = 7 Hz, $^3J(^1H,^{31}P)$ = 20 Hz, 12H; CH(C*H*$_3$)$_2$]; $^{13}C\{^1H\}$ NMR: δ = 33.2 (m, 4C; *C*H(CH_3)$_2$), 18.6 (s, 4C; CH(*C*H$_3$)$_2$), 17.7 (s, 4C; CH(*C*H$_3$)$_2$); $^{31}P\{^1H\}$ NMR: δ = 92.8 [s, $^1J(^{77}Se,^{31}P)$ = 440 Hz, $^2J(^{31}P,^{31}P)$ = 34 Hz]; ^{77}Se NMR: δ = 297 (br, d, $^1J(^{77}Se,^{31}P)$ = 430 Hz). UV-Vis (CH_2Cl_2): 230-270 and 365 nm ($\varepsilon = 1.7*10^4$ $mol^{-1}cm^{-1}$).

Spectroscopic data of [N(P^{i}Pr$_2$Te)$_2$]I (5).[16] ^{1}H NMR (D_8-THF, 23 °C): δ = 2.62 [2 x sept., $^3J(^1H,^1H)$ = 7 Hz, 4H; C*H*(CH_3)$_2$], 1.35 [dd, $^3J(^1H,^1H)$ = 7 Hz, $^3J(^1H,^{31}P)$ = 18 Hz, 12H; CH(C*H*$_3$)$_2$], 1.31 [dd, $^3J(^1H,^1H)$ = 7 Hz, $^3J(^1H,^{31}P)$ = 20 Hz, 12H; CH(C*H*$_3$)$_2$]; $^{13}C\{^1H\}$ NMR: δ = 33.1 (m, 4C; *C*H(CH_3)$_2$), 19.6 (s, 4C; CH(*C*H$_3$)$_2$), 18.1 (br, s, 4C; CH(*C*H$_3$)$_2$); $^{31}P\{^1H\}$ NMR: δ = 68.1 [s, $^1J(^{125}Te,^{31}P)$ = 1040 Hz, $^2J(^{31}P,^{31}P)$ = 31 Hz]. UV-Vis (CH_2Cl_2): 230-270 and 365 nm ($\varepsilon = 3.7*10^4$ $mol^{-1}cm^{-1}$).

Synthesis of [N(P^{i}Pr$_2$Se)$_2$]SbF$_6$ (6). A solution of **4** (0.213 g, 0.40 mmol) in 25 mL of toluene was cooled to -80 °C and a solution of $AgSbF_6$ (0.137 g, 0.40 mmol) in 25 mL of toluene was added slowly via cannula. The reaction mixture was stirred for 1 h at -80 °C and 2 h at 23 °C. Solvent was evaporated under vacuum and the resulting orange precipitate was dissolved to

ca. 50 ml of THF. AgI was allowed to settle and the solution was filtered through a microfilter (0.45 μm PTFE) and then dried under vacuum yielding an orange, slightly sticky powder (0.200 g, 78 %). Elemental analysis calcd (%) for $C_{12}H_{28}F_6N_1P_2Sb_1Se_2$: C 22.45, H 4.40, N 2.18; found: C 23.21, H 4.47, N 2.31. ^{1}H NMR (D_8-THF, 23 °C): δ = 2.82 [2 x sept., $^3J(^1H,^1H)$ = 7 Hz, 4H; C*H*$(CH_3)_2$], 1.42 [dd, $^3J(^1H,^1H)$ = 7 Hz, $^3J(^1H,^{31}P)$ = 20 Hz, 12H; CH(C*H*$_3)_2$], 1.40 [dd, $^3J(^1H,^1H)$ = 7 Hz, $^3J(^1H,^{31}P)$ = 21 Hz, 12H; CH(C*H*$_3)_2$]; $^{13}C\{^1H\}$ NMR: δ = 31.4 (m, 4C; *C*H$(CH_3)_2$), 17.7 [s, 4C; CH(*C*H$_3)_2$], 17.4 [s, 4C; CH(*C*H$_3)_2$]; $^{31}P\{^1H\}$ NMR: δ = 113.2 [s, $^1J(^{77}Se,^{31}P)$ = 363 Hz, $^2J(^{31}P,^{31}P)$ = 45 Hz]; ^{77}Se NMR: δ = 344 [d, $^1J(^{77}Se,^{31}P)$ = 360 Hz]. UV-Vis (CH_2Cl_2): λ 230-270 and 365 nm (ε = 1.1*10^3 mol^{-1}cm^{-1}). X-ray quality crystals were obtained by layering toluene on top of a THF solution of **6**.

Synthesis of [N(P^{i}Pr$_2$Te)$_2$]SbF$_6$ (7). The salt **7** was obtained as a dark blue, slightly sticky powder (0.235 g, 80 %) from the reaction of **5** (0.252 g, 0.40 mmol) in 25 mL of toluene with $AgSbF_6$ (0.137 g, 0.40 mmol) in 25 mL of toluene by using a procedure identical to that described above for **6**. Elemental analysis calcd (%) for $C_{12}H_{28}F_6N_1P_2Sb_1Te_2$: C 19.50, H 3.82, N 1.89; found: C 20.16, H 3.86, N 2.01. ^{1}H NMR (D_8-THF, 23 °C): δ = 2.64 [2 x sept., $^3J(^1H,^1H)$ = 7 Hz, 4H; C*H*$(CH_3)_2$], 1.37 [dd, $^3J(^1H,^1H)$ = 7 Hz, $^3J(^1H,^{31}P)$ = 19 Hz, 12H; CH(C*H*$_3)_2$], 1.34 [dd, $^3J(^1H,^1H)$ = 7 Hz, $^3J(^1H,^{31}P)$ = 21 Hz, 12H; CH(C*H*$_3)_2$]; $^{13}C\{^1H\}$ NMR: δ = 32.3 (m, 4C; *C*H$(CH_3)_2$), 19.1 [s, 4C; CH(*C*H$_3)_2$], 18.0 [s, 4C; CH(*C*H$_3)_2$]; $^{31}P\{^1H\}$ NMR: δ = 85.7 [s, $^1J(^{125}Te,^{31}P)$ = 863 Hz, $^2J(^{31}P,^{31}P)$ = 39 Hz]; ^{125}Te NMR: δ = 254 [d, $^1J(^{125}Te,^{31}P)$ = 870 Hz]. UV-Vis: λ 230-270 and 365 nm (ε = 3.6*10^3 mol^{-1}cm^{-1}), and 595 nm (ε = 190 mol^{-1}cm^{-1}) in CH_2Cl_2; λ 230-270 and 365 nm (ε = 3.2*10^3 mol^{-1}cm^{-1}), and 560 nm (ε = 200 mol^{-1}cm^{-1}) in MeCN. X-ray quality crystals were grown by layering n-hexane on top of a THF solution of **7**.

Formation of [N(P^{i}Pr$_2$Te)$_2$]Cl (8). A few X-ray quality crystals of **8** were obtained from the reaction solution of an equimolar reaction between $[N(P^iPr_2Te)_2]_2$ and SO_2Cl_2 in toluene. The reaction yielded a complex mixture of products, as shown by the ^{31}P NMR spectroscopy, and therefore the compound **8** was not obtained as pure product in reasonable yield.

Synthesis of [N(PPh$_2$Te)$_2$]I (9). A solution of [(TMEDA)NaN(PPh$_2$Te)$_2$] (0.389 g, 0.50 mmol) in 35 mL of toluene was cooled to -80 °C and a solution of I_2 (0.127 g, 0.50 mmol) in 15 mL of THF was added slowly via cannula. The resulting red solution was stirred for 1 h at -80 °C and 2 h at 23 °C. A dark red precipitate was allowed settle and the orange solution was decanted via cannula. The precipitate was dried under vacuum and then washed with MeCN affording **9** as red-brown powder (0.253 g, 66 %). Elemental analysis calcd (%) for $C_{24}H_{20}I_1N_1P_2Te_2$: C 37.61, H 2.63, N 1.83; found: C 36.91, H 2.45, N 1.75. ^{1}H NMR (CD_2Cl_2, 23 °C): δ = 7.76 (m), 7.57 (m), 7.46 (m); ^{31}P{^{1}H} NMR: δ = 21.9 [s, $^1J(^{125}Te,^{31}P)$ = 1066 Hz]. X-ray quality crystals of **9** were grown from CH_2Cl_2.

Reaction of [(TMEDA)NaN(PPh$_2$Se)$_2$] with I$_2$. A slurry of [(TMEDA)NaN(PPh$_2$Se)$_2$] (0.273 g, 0.40 mmol) in 35 mL of n-hexane was cooled to -80 °C and a solution of I_2 (0.102 g, 0.40 mmol) in 15 mL of toluene was added slowly via cannula. The resulting red solution was stirred for 1 h at -80 °C and 2 h at 23 °C. The precipitate was allowed settle and the orange-yellow solution was decanted via cannula. The precipitate was dried under vacuum and then washed with MeCN affording an orange-yellow powder (0.241 g, 90 % in n-hexane/toluene, calculated as a 1:1 mixture of **10** and **11**). A slightly lower yield was obtained when the reaction was carried out in an n-hexane/THF mixture. ^{31}P{^{1}H} NMR (D_8-THF, 23 °C): δ = 49.5 [s, br, $^1J(^{31}P,^{77}Se)$ = 447 Hz] (**10**), δ = 36.1 [s, $^1J(^{77}Se,^{31}P)$ = 745 Hz] (**11**), δ = 24.3 (s) (**11**). X-ray quality crystals of **10** were grown from CH_2Cl_2. Attempts to grow X-ray quality crystals of **11** from CH_2Cl_2 produced crystals of the hydrolysis product **12**.

Reaction of [(TMEDA)NaN(P^{i}Pr$_2$Se)$_2$] with SeCl$_2$. A freshly prepared solution of $SeCl_2$ (0.039 g red selenium and 0.067g SO_2Cl_2, 0.50 mmol)[18] in *ca.* 1 mL of THF was added to a slurry of [(TMEDA)NaN(P^{i}Pr$_2$Se)$_2$] (0.273 g, 0.50 mmol) in *ca.* 40 mL of n-hexane at -80 °C. The reaction mixture was stirred for 1 h at -80 °C and 2 h at 23 °C resulting in a pale yellow solution and a mixture of red and white powders. The solution was decanted via cannula and, after several days at -20 °C, produced colorless crystals of [SeP(^{i}Pr$_2$)N(^{i}Pr$_2$)PCl] (**13**) (0.071 g,

39 %). The main component of the powders (0.148 g) was shown to be **13** by ^{31}P NMR spectroscopy. Elemental analysis calcd (%) for $C_{14}H_{28}Cl_1N_1P_2Se_1$: C 39.74, H 7.78, N 3.86; found: C 39.94, H 7.90, N 4.51. ^{1}H NMR (D_8-THF, 23 °C): δ = 2.71 [2 x sept., $^{3}J(^{1}H,^{1}H)$ = 7.1 Hz, 4H; C*H*$(CH_3)_2$], δ = 2.02 [2 x sept., $^{3}J(^{1}H,^{1}H)$ = 6.9 Hz, 4H; C*H*$(CH_3)_2$], 1.36 [dddd, $^{3}J(^{1}H,^{31}P)$ = 20.0 Hz, $^{3}J(^{1}H,^{1}H)$ = 7.1 Hz, 6H; CH(C*H*$_3)_2$], 1.15 [dd, $^{3}J(^{1}H,^{31}P)$ = 17.1 Hz, $^{3}J(^{1}H,^{1}H)$ = 6.9 Hz, 6H; CH(C*H*$_3)_2$]; ^{13}C{^{1}H} NMR: δ = 33.0 [m, 2C; *C*H$(CH_3)_2$)], δ = 33.2 [m, 2C; *C*H$(CH_3)_2$)], 17.6 [s, 2C; CH(*C*H$_3)_2$], 17.1 [m, 4C; CH(*C*H$_3)_2$], 16.9 [m, 2C; CH(*C*H$_3)_2$]; ^{31}P{^{1}H} NMR: δ = 67.2 [d, $^{1}J(^{77}Se,^{31}P)$ = 722 Hz, $^{2}J(^{31}P,^{31}P)$ = 37 Hz], δ = 66.0 [d, $^{2}J(^{31}P,^{31}P)$ = 37 Hz]; ^{77}Se NMR: δ = -308 [d, $^{1}J(^{77}Se,^{31}P)$ = 722 Hz].

X-ray Crystallography. Crystals of **6**, **7, 8**, **9**, **10**, **12** and **13** were coated with Paratone 8277 oil and mounted on a glass fiber. Diffraction data were collected on a Nonius KappaCCD diffractometer using monochromated Mo K$_\alpha$ radiation (λ = 0.71073 Å) at -100 °C. The data sets were corrected for Lorentz and polarization effects, and empirical absorption correction was applied to the net intensities. The structures were solved by direct methods using SHELXS-97 [19] and refined using SHELXL-97.[20] After the full-matrix least-squares refinement of the non-hydrogen atoms with anisotropic thermal parameters, the hydrogen atoms were placed in calculated positions [C-H = 1.00 Å for C*H*$(CH_3)_2$, 0.98 Å for CH(C*H*$_3)_2$ and 0.95 Å for Phenyl hydrogens]. The isotropic thermal parameters of the hydrogen atoms were fixed at 1.2 times to that of the corresponding carbon for C*H*$(CH_3)_2$ and Phenyl hydrogens, and 1.5 times for CH(C*H*$_3)_2$. In the final refinement the hydrogen atoms were riding with the carbon atom to which they were bonded. The scattering factors for the neutral atoms were those incorporated with the programs. Crystallographic data are summarized in Table 1.

Computational Details. DFT calculations were performed primarily for compounds **3b** and **3c**. The molecular structures were optimized by using a combination of the hybrid PBE0 exchange-correlation functional[21] with the Ahlrichs' triple-zeta valence basis set augmented by

one set of polarization functions (TZVP); [22] for tellurium, the corresponding ECP basis set was used. Excitation energies were calculated using the TDDFT formalism; the same density functional-basis set combination as used in the geometry optimizations was utilized. All calculations were performed with Turbomole 5.8[22] and Gaussian 03[23] program packages.

Results and Discussion

Synthesis of 6 and 7. The hexafluoroantimonate salts **6** and **7** are readily obtained in excellent yields by the reactions of **4** and **5**, respectively, with $AgSbF_6$ in a 1:1 molar ratio in toluene (eq.1).

$$[N(P^iPr_2E)_2]I + AgSbF_6 \rightarrow [N(P^iPr_2E)_2]SbF_6 + AgI \quad (1)$$

[E = Se (**6**), Te (**7**)]

The multinuclear NMR spectra of **6** and **7** reveal very similar features to those observed for the corresponding iodide salts **4** and **5**.[16] The $^{31}P\{^1H\}$ NMR spectra of **6** and **7** are comprised of a singlet at δ 113.2 and 85.7, respectively, with a set of ^{77}Se and ^{125}Te satellites arising from the AA′X spin system of magnetically inequivalent phosphorus atoms. Similarly to **4** and **5**, the singlets observed for both **6** and **7** do not resolve into two doublets even at low temperature (-100 °C), indicating a weak interaction of the anion with the cyclic cation that is symmetrical with respect to the chalcogen-chalcogen bond in solution.[24] This conclusion is supported by the ^{77}Se and ^{125}Te NMR spectrum of **6** and **7**, which exhibit a doublet at δ 344 [$^1J(^{77}Se,^{31}P)$ = 360 Hz] and a doublet at δ 254 [$^1J(^{125}Te,^{31}P)$ = 870 Hz], respectively, consistent with a single chalcogen environment in each case. The ^1H NMR spectra of **6** and **7** display two overlapping sets of septets (appearing as an octet) for the CH-hydrogens and two sets of doublets of doublets for the CH_3-hydrogens. Consistently, the $^{13}C\{^1H\}$ NMR spectra show a multiplet for the α-carbons of

the $CH(CH_3)_2$ groups and two singlets for the CH_3-carbons indicating two inequivalent isopropyl groups. Taken together, these NMR data suggest that the cationic five-membered rings in **4**-**7** retain their non-planar structures and C_2 symmetry in solution.

The replacement of the I^- counter-ion by SbF_6^- results in a shift of the ^{31}P NMR resonances to higher frequency by *ca.* 20 ppm for both the selenium- and tellurium-containing cations, indicating decreased shielding for the phosphorus atoms in the hexafluoroantimonate salts**.** A shift to higher frequency is also observed for the doublet in the ^{77}Se NMR spectra of **4** and **6** (δ 297 and 344, respectively). The replacement of the I^- counter-ion by SbF_6^- also results in a decrease in the magnitude of the $^1J(^{77}Se,^{31}P)$ and $^1J(^{125}Te,^{31}P)$ coupling constants from 440 to 360 Hz and from 1040 and 870 Hz for the selenium and tellurium-containing cations, respectively. At the same time, the $^2J(^{31}P,^{31}P)$ coupling constants increase slightly (by *ca*. 10 Hz).

Crystal structures of 4-8. The molecular structures of **4**-**8** with the atomic numbering schemes are depicted in Figure 1 and selected bond parameters are summarized in Table 2. The compounds **4**-**8** are comprised of non-planar, five-membered $[N(P^iPr_2E)_2]^+$ rings and counter anions, which interact primarily with one of the chalcogens. While the structures of **4** and **5** exhibit infinite chains of cations linked by chalcogen-iodine contacts (Figure 1a),[16] the compounds **6**-**8** are comprised of centrosymmetric ion pairs, with chalcogen-chalcogen close contacts and chalcogen-halogen interactions (Figure 1b-d). The dimeric SbF_6^- salts **6** and **7** exhibit similar structural features (Figure 1b and c), but their crystal packing and crystal systems are distinct. As illustrated in Figure 2, the dimeric units in **6** are arranged in a linear fashion along the *c* axis whereas these units adopt a herringbone stacking pattern in the tellurium analog **7**. These disparities are attributed to a slightly different orientation of the SbF_6^- anion; whereas **6** shows two Se···F contacts [2.982(3) and 3.329(2) Å], the tellurium system **7** exhibits only one Te···F contact [3.120(4) Å]. Interestingly, the crystals of **7** also display a significant pleochroism by having either a purple-red or a blue color depending on the orientation of the crystal (under

both polarized and non-polarized light). The color of the crystals of **6**, however, is independent of the crystal orientation. The pleochroism in **7** is tentatively attributed to the different packing arrangement of the dimeric units.

The most significant structural feature of **4** and **5** is the unusually long chalcogen-chalcogen bond [2.4839(9) and 2.8387(9) Å, respectively] [16] compared to the related six π-electron, five-membered cyclic cations in the salts $[PhCN_2Se_2][PF_6]$ [25a] and $[Se_3N_2][AsF_6]_2$ [25b] [Se-Se: 2.260(5) and 2.334(3) Å, respectively], and to the Te-Te bond length in the cation $[(Te_2SN_2)Cl]^+$, in which one of the Te atoms is three-coordinate [2.731(2) Å].[26] The Se-Se bond length is also significantly longer than the value of 2.4044(8) Å observed in the neutral heterocycle $Se_3(NAd)_2$, which is also a puckered five-membered ring.[27] DFT calculations[16] indicate that this elongation results from donation of electron density from a lone pair of the iodide counter-ion into the E-E σ* orbital (LUMO) of the cation, *cf*. formation of triiodide I_3^- anion from an I^- ion and an I-I molecule.[28] The structural features of the chloride salt $[N(P^iPr_2Te)_2]Cl$ (**8**) are consistent with this interpretation by showing an even longer Te-Te bond [2.9026(7) Å] than that observed in **5** as a result of the stronger halide-chalcogen interaction. As indicated in Table 2, the calculated Te···Cl bond order in **8** is 0.35 while the Te···I bond order in **5** is only 0.09.[30] Consistently, the ion-separated salts **6** and **7**, which exhibit only very weak ionic interactions (the E···F bond order is *ca.* 0.02 for both **6** and **7**),[30] display chalcogen-chalcogen bond lengths that are typical of single bonds [Se-Se: 2.348(7) Å in **6** and Te-Te: 2.7162(7) Å in **7**]. These values are also in excellent agreement with the calculated values of 2.364 Å and 2.726 Å for the bare cations **3b** and **3c**, respectively.

While the halide-chalcogen interactions result in a significant disparity (of 0.04 – 0.06 Å) in the P-E bond lengths in **4**, **5** and **8**, the corresponding distances in **6** and **7** show very small differences of *ca*. 0.01 Å. Changing the anion from a halide to SbF_6^- has very little effect on the average P-E and P-N bond lengths. The mean P-Se distances are 2.25 and 2.26 Å in **4** and **6**,

respectively, and the P-Te bond lengths are 2.41, 2.49 and 2.47 Å in **5**, **7** and **8**, respectively. The mean P-N bond lengths in compounds **4**-**8** span the narrow range of 1.589-1.594 Å.

The average P-N-E bond angles in **4**-**8** are close to the ideal tetrahedral values, varying from 107.3° in **6** to 110.9° in **8**. A P1-E1-E2-P2 dihedral angle of *ca.* 25.6° is observed for the halide salts **4**, **5** and **8**, while the SbF_6^- salts show a slightly larger value of *ca.* 28.6°. The P-E-E bond angles are more dependent on the strength of the anion interaction to one of the two chalcogens. Thus, **4** and **8** show a difference of *ca.* 2.5° and 2.0° between the P1-E1-E2 and P2-E2-E1 angles, respectively, whereas the corresponding difference in the SbF_6^- salts **6** and **7** is only *ca.* 1°. The P-E-E angles in **5** are equal within experimental error due to the two almost identical Te···I close contacts in the solid state [Te1···I1: 3.430(1) Å and Te2···$I1^a$: 3.494(1) Å]. Expectedly, the elongation of the chalcogen-chalcogen bond has a noticeable effect on the P-N-P angles, which are somewhat wider in the halide salts **4**, **5** and **8** than in the hexafluoroantimonate salts **6** and **7**.

In the Raman spectrum of **4** the most intense band at 195 cm^{-1} is attributed to the Se-Se stretching vibration, which is shifted to 255 cm^{-1} in **6** reflecting the decrease in the Se-Se bond length. Both of these Raman lines correlate well with, for example, the ν(Se-Se) stretching vibration at 269 cm^{-1} observed for $[(Se_2SN_2)Cl]_2$, which exhibits a Se-Se bond length of 2.3464(7) Å.[32] The Te-Te stretching vibrations show similar behavior; the most intense Raman line at 149 cm^{-1} observed for **5** shifts to 165 cm^{-1} for **7**. The latter value can be compared to the band at 167 cm^{-1} observed for diphenyl ditelluride $(PhTe)_2$[33] which has a Te-Te bond length of 2.712(2) Å.[34]

UV-Visible spectra. The assignments of the absorptions observed in the UV-Visible spectra of compounds **4**-**7** were guided by the TDDFT excitation energy calculations carried out for the bare cations **3b** and **3c**. The selenium-containing **4** and **6** exhibit broad absorptions in the region 230-270 and at 365 nm in CH_2Cl_2, as well as a "tail" with a significantly lower molar absorptivity at *ca.* 450 nm as expected from the yellow-orange color of solutions. The absorption

in the visible region is attributed to the HOMO→LUMO transition (π*→σ*, Figure 3) and is computationally predicted to appear at 460 nm. The calculations for **3b** also show several transitions in the 230-270 nm region; those with the highest oscillator strength correspond to the HOMO-4→LUMO (σ→σ*), HOMO→LUMO+2 (π*→σ*) and HOMO-1→LUMO+1 (π^{NB}→σ*) transitions.

The tellurium-containing compounds **5** and **7** exhibit broad absorptions at *ca.* 230-270 and 365 nm, and **7** also shows a weak absorption at 560 nm in MeCN that shifts to 595 nm in CH_2Cl_2, reflecting the different colors of these solutions (purple-red in MeCN and greenish-blue in CH_2Cl_2). Like the selenium compounds **4** and **6**, the visible absorption band is attributed to the HOMO→LUMO transition (π*→σ*, Figure 3) and is computationally predicted to occur at 554 nm. The most significant transitions in the 230-270 nm region are HOMO-2→LUMO+1 (π→σ*), HOMO→LUMO+2 (π*→σ*) and HOMO-1→LUMO+2 (π^{NB}→σ*).

Surprisingly, the calculations predict no excitations at *ca.* 365 nm, although bands in this region with high molar absorptivities are observed experimentally. In compounds **4**-**7** these absorptions are tentatively attributed to cation-anion interactions, which were not included in the calculations. This hypothesis is supported by the observation that the molar absorptivity for the 365 nm band decreases by an order of ten when the counter-ion is changed from I^- to SbF_6^-. Furthermore, TDDFT calculations for **5,** with variation of the Se···I distances, reveal the appearance of new transitions in the 320-380 nm range. As expected, these transitions have relatively high predicted oscillator strengths and involve excitations from the inner occupied MOs centered mostly on the halogen atom to the Se-Se-I antibonding LUMO of the complex. The inclusion of a counter-ion also has an influence on the calculated HOMO→LUMO transitions. Although the excitation energy remains essentially unchanged at 460 ± 10 nm, a significant decrease in the oscillator strength is predicted. These findings are consistent with the observation that transitions in the visible region of the spectrum are only observed for compounds **5** and **7**, and not for **4** and **6**.

Synthesis and structure of 9. The reaction between the phenyl-substituted [(TMEDA)NaN($PPh_2Te)_2$] and I_2 produces [$N(PPh_2Te)_2$]I **(9)** as a red-brown powder. However, the yield of **9** is 66%, significantly lower than the 92% yield achieved for the isopropyl analog **5**.[16] Complex **9** was characterized by multinuclear NMR spectra and, after recrystallization from CH_2Cl_2, by a single crystal X-ray structural determination. The $^{31}P\{^1H\}$ NMR spectrum of **9** in CH_2Cl_2 consists of a singlet at 21.9 ppm with ^{125}Te satellites ($^1J(^{125}Te,^{31}P)$ = 1066 Hz, *cf*. 1040 Hz for **5**). In contrast to the isopropyl derivatives **4**-**7**, the two bond ^{31}P-^{31}P coupling is not resolved for **9** owing to the significantly broader signals. The ^{125}Te NMR signal could not be observed because of the low solubility of **9**.

The structural features of the five-membered cyclic cation in **9** (Figure 4a) resemble those of the isopropyl derivative **5**. Selected bond parameters are given in Table 2. In contrast to **5**, however, the phenyl derivative **9** exists as a centrosymmetric ion pair with a significantly shorter Te···I close contact than that observed in **5** (3.169(1) Å in **9** vs. 3.430(1) Å in **5**). Despite the stronger Te···I interaction, the Te-Te bond lengths in **9** and **5** of 2.846(1) Å and 2.840(1) Å, respectively, are indistinguishable. The P-Te bonds in **9** are *ca*. 0.07 Å longer than those observed in **5**, but are close to the corresponding bond lengths in the chloride salt **8**. In addition, the five-membered rings in **5** and **8** are slightly more puckered than that in **9** as reflected in the larger (by *ca*. 4.7°) P1-Te1-Te2-P2 dihedral angle.

The reaction of [(TMEDA)NaN($PPh_2Se)_2$] with I_2. In contrast to the successful preparation of the tellurium-containing compound **9**, the attempted synthesis of the selenium analog, [$N(PPh_2Se)_2$]I, by the reaction of [(TMEDA)NaN($PPh_2Se)_2$] and I_2 in a 1:1 molar ratio afforded an equimolar mixture of [$N(PPh_2Se)_2$(μ-Se)][I] (**10**) and [$SeP(Ph_2)N(Ph_2)PI$] (**11**).

The identity of **10** was determined by an X-ray structural determination. The molecular structure with the atomic numbering scheme is depicted in Figure 4b and the relevant bond parameters are summarized in Table 3. The structure of **10** consist of a centrosymmetric dimer formed by two cyclic six-membered cations in chair conformation and two bridging I^- anions.[35]

The Se3 atom exhibits two similar Se···I close contacts [Se3···I1 3.102(1) and Se3···I1^{b} 3.140(1) Å] and two almost equal Se-Se bond lengths [Se1-Se3 2.441(1) and Se2-Se3 2.427(1) Å] resulting in a slightly distorted square plane. The mean Se-Se distances are *ca*. 0.21 Å shorter than those observed in the square-planar complex {[N(P^{i}Pr$_2$Se)$_2$]$_2$(μ-Se)},[37] which can be described as consisting of two [N(P^{i}Pr$_2$Se)$_2$]$^-$ anions chelated to a central Se^{2+} cation.[37] The stronger interaction of a single [N(P^{i}Pr$_2$Se)$_2$]$^-$ anion with a Se^{2+} cation may explain the shorter Se-Se bond lengths in **10**. The Se-Se bond lengths and Se···I close contacts in the dimer **10** are comparable to those observed in the iodide salt of the five-membered cyclic cation **4**. The Se-P and P-N bond lengths are also similar to those found in the five-membered rings **4** and **6**. The more open Se1-P1-N1-P2-Se2 unit in **10** compared to the closed cyclic structure in **4** and **6** is reflected in both the P-N-P and N-P-Se bond angles, which are *ca.* 5° and 8° wider in **10** than in **4** and **6**, respectively. The crystal packing in **10** results in planar arrangement of two of the phenyl groups with the nitrogen atom located between the rings (Figure 5).

The identity of the second product [SeP(Ph$_2$)N(Ph$_2$)PI] (**11**) was established by an X-ray structural determination of the hydrolysis product {[N(PPh$_2$)$_2$Se]$_2$(μ-O)}•CH$_2$Cl$_2$ (**12**•CH$_2$Cl$_2$) and is supported by the ^{31}P NMR data (see discussion below). The crystal structure determination of **12**•CH$_2$Cl$_2$[38] (Figure 4c) revealed a nine atom Se-P-N-P-O-P-N-P-Se chain with selenium atoms in a *cis* configuration. Selected bond parameters for **12**•CH$_2$Cl$_2$ are given in Table 3. The Se-P bond length [2.117(1) Å] is comparable to the value of 2.120(2) Å observed for the terminal P=Se bonds in the eight atom chain [Se=P(Ph$_2$)N(Ph$_2$)P-P(Ph$_2$)N(Ph$_2$)P=Se].[40] The significant difference between the P1-N1 [1.620(3) Å] and P2-N1 [1.549(3) Å] bond lengths is consistent with the bonding arrangement for **12** depicted in Scheme 1.

Formation of 10 and 12. The reaction of [(TMEDA)NaN(PPh$_2$Se)$_2$] and I$_2$ in a 1:1 molar ratio was repeated several times and the ^{31}P{^{1}H} NMR spectrum of the product mixture was comprised consistently of three singlets at δ 49.5, 36.1 and 24.3 with an intensity ratio of 2:1:1, respectively. The broad resonance at δ 49.5 shows ^{77}Se satellites. The magnitude of the

coupling constant $^{1}J(^{31}P,^{77}Se)$ = 447 Hz implies a P-Se bond order of about 1 [41] and, hence, this resonance is attributed to the cyclic cation in **10**. Although the two singlets at δ 36.1 and 24.3 do not exhibit ^{31}P-^{31}P coupling, these resonances consistently appeared with 1:1 relative intensities and, therefore, they are assumed to arise from a single compound. The former resonance exhibits ^{77}Se satellites with $^{1}J(^{31}P,^{77}Se)$ = 745 Hz, which is consistent with a terminal P=Se bond,[41] while the latter resonance exhibits no ^{77}Se satellites. In the light of these NMR data, we tentatively suggest that **11** is the acyclic compound [SeP(Ph$_2$)N(Ph$_2$)PI]. As indicated in Scheme 1, the hydrolysis of this species during recrystallization gives rise to the structurally characterized nine atom chain **12**. [42, 43]

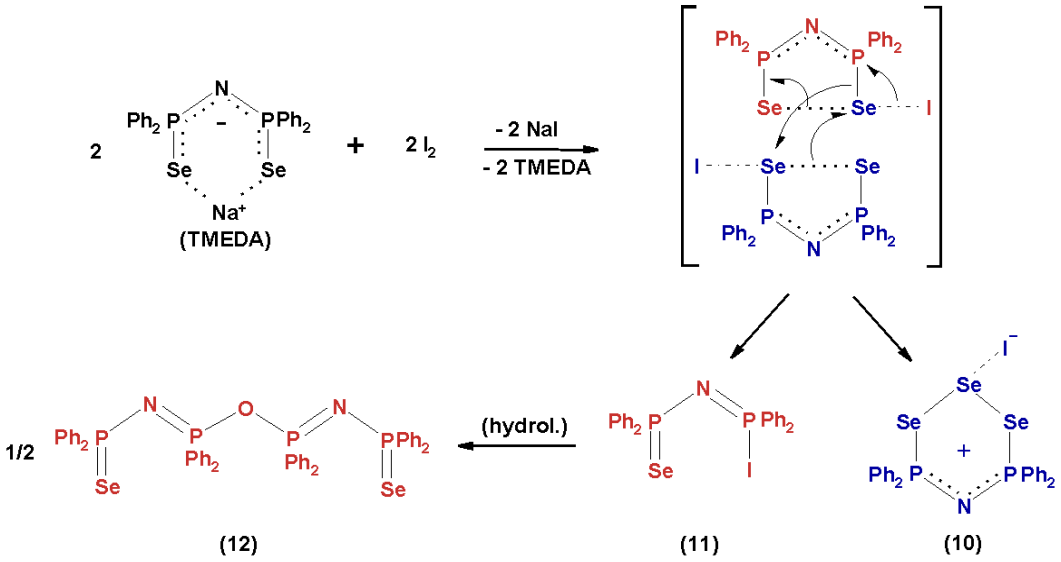

Scheme 1.

In order to explain the formation of equimolar amounts of **10** and **11** in the reaction of [(TMEDA)NaN(PPh$_2$Se)$_2$] and I$_2$, we propose the initial formation of the five-membered ring, [N(PPh$_2$Se)$_2$]$^+$, and subsequent decomposition of this cyclic cation by an intermolecular process (Scheme 1). In order to provide some insight into the occurrence of this decomposition process for [N(PPh$_2$Se)$_2$]$^+$, but not for the tellurium analog [N(PPh$_2$Te)$_2$]$^+$, DFT calculations of the formation energies of a 1:1 mixture of the two products [N(PR$_2$E)$_2$(μ-E)][I] and [EP(R$_2$)N(R$_2$)PI] (E = Se, Te; R = H, ^{i}Pr, Ph) were carried out. The conversion of two molecules of [N(PPh$_2$Se)$_2$]I

into **10** and **11** was found to be approximately thermoneutral in the gas phase, whereas the analogous process for **4**, **5** and **9** is endothermic by *ca.* 55, 85 and 50 kJ mol^{-1}, respectively; the calculated reaction energies for the hypothetical R = H structures were highly endothermic (> 100 kJ mol^{-1}). Although these calculations do not consider the kinetic aspects of the reaction or the relative lattice energies of salts containing the five- or six-membered cyclic cations, the trend in formation energies is nevertheless consistent with the experimentally observed decomposition of $[N(PPh_2Se)_2]I$. It is conceivable that the instability of the five-membered ring in this case results from an enhancement of the $I^- \rightarrow Se\text{-}Se(\sigma^*)$ electron transfer caused by the electron-withdrawing phenyl substituents on phosphorus and a concomitant weakening of the Se-Se bond.

Formation and structure of [SeP(^{i}Pr$_2$)N(^{i}Pr$_2$)PCl] (13). The reaction of $[(TMEDA)NaN(P^iPr_2Se)_2]$ with $SeCl_2$ was carried out in a 1:1 molar ratio in an attempt to generate the isopropyl derivative of the six-membered ring in **10** as the chloride salt. However, instead of the expected product, the acyclic compound $[SeP(^iPr_2)N(^iPr_2)PCl]$ **(13)** was obtained in 39% yield (eq. 2). This unsymmetrical derivative was characterized by multinuclear NMR spectra and by an X-ray structural determination.[44]

$$[(TMEDA)NaN(P^iPr_2Se)_2] + SeCl_2 \rightarrow [SeP(^iPr_2)N(^iPr_2)PCl] + NaCl + TMEDA + \tfrac{1}{4}\, Se_8 \qquad (2)$$

The $^{31}P\{^1H\}$ NMR spectrum of **13** is comprised of two mutually coupled doublets at δ 67.2 and 66.0 with $^2J(^{31}P,^{31}P)$ = 37 Hz. The former resonance shows ^{77}Se satellites with $^1J(^{77}Se,^{31}P)$ = 722 Hz, cf. 745 Hz in **11**, consistent with a terminal P=Se bond.[41] The $^{77}Se\{^1H\}$ NMR spectrum of **13** exhibits a doublet at δ -308 with $^1J(^{77}Se,^{31}P)$ = 722 Hz. As expected for this unsymmetrical derivative, the $^{13}C\{^1H\}$ and ^1H NMR spectra exhibit resonances that are more widely separated than those observed for **4**-**8** owing to the significant difference in the environments of the isopropyl groups in **13**.

The molecular structure of **13** (Figure 6) shows a *cis* arrangement for the terminal selenium and chlorine atoms of the distorted SePNPCl chain similar to the configuration of the selenium atoms in the symmetrical derivative [SeP(^{i}Pr$_2$)NH(^{i}Pr$_2$)PSe].[7] Selected bond parameters for **13** are summarized in Table 3. The Se=P bond length [2.125(1) Å] is comparable to the values of 2.117(1), *ca.* 2.10 and 2.120(2) Å found in **12**, [SeP(^{i}Pr$_2$)NH(^{i}Pr$_2$)PSe][7] and [Se=P(Ph$_2$)N(Ph$_2$)P-P(Ph$_2$)N(Ph$_2$)P=Se],[40] respectively. The difference between the P1-N1 and P2-N1 bond lengths of *ca.* 0.1 Å is comparable to that observed in **12** and suggests a trend towards single and double bond character for the two P-N bonds, respectively. The P-N-P bond angle in **13** (147.0(2)°) is substantially wider than the values of 135.6(2), 131.2(2) and 135.5(4)° observed in **12**, [SeP(^{i}Pr$_2$)NH(^{i}Pr$_2$)PSe][7] and [Se=P(Ph$_2$)N(Ph$_2$)P-P(Ph$_2$)N(Ph$_2$)P=Se].[40] Although the P-N-P-Se dihedral angles in **12** and **13** are identical, **13** shows a less puckered chain than that of **12** [τ P-N-P-Cl in **13** is 43.5(5)° and τ P-N-P-O in **12** is 63.3(3)°]. In the crystal lattice (see Figure S2 in Supporting Information), **13** forms molecular strands connected by Cl···H close contacts [2.883(1) Å] that are slightly shorter than the sum of van der Waals radii (2.95 Å).[31]

Conclusions

The synthesis and structural characterization of the SbF_6^- salts of the cyclic cations $[N(P^iPr_2E)_2]^+$ (E = Se, Te) has provided experimental verification for the earlier suggestion, based on DFT calculations,[16] that the unusually long chalcogen-chalcogen bonds observed in the corresponding iodide salts can be attributed primarily to the donation of electron density from an electron pair of the halide anion into the E-E σ* orbital (LUMO) of the ring system. Changing the substituent on phosphorus from isopropyl to the electron-withdrawing phenyl has an unanticipated influence on the outcome of the oxidation of the $[N(PR_2E)_2]^-$ anion (E = Se, Te). The tellurium-containing cation, $[N(PPh_2Te)_2]^+$, was obtained as the iodide salt, albeit in

significantly lower yield than the analogous isopropyl derivative. By contrast, the attempted synthesis of the selenium analog $[N(PPh_2Se)_2]^+$ produced a 1:1 mixture of a novel six-membered ring, $[N(PPh_2Se)_2(\mu\text{-}Se)][I]$, and an acyclic species $[SeP(Ph_2)N(Ph_2)PI]$. DFT calculations support the suggestion that these products are formed by the decomposition of the initially formed five-membered ring $[N(PPh_2Se)_2]^+$ cation. The reaction of $[(TMEDA)NaN(P^iPr_2Se)_2]$ with $SeCl_2$ unexpectedly afforded, as the main product, the acyclic compound $[SeP(^iPr_2)N(^iPr_2)PCl]$, a potentially useful reagent for the construction of chains or macrocycles in view of the reactive P-Cl functionality.

Acknowledgments. The authors gratefully acknowledge financial support from the Academy of Finland (J.K. and H.M.T.) and the Natural Sciences and Engineering Research Council (Canada). We are also thankful for Professor Michael Gerken (Univ. of Lethbridge) for obtaining the Raman spectra.

Supporting information available: X-ray crystallographic files in CIF format, vibrational data (IR and Raman) for compounds **4**-**7**, **9** and **13** (Table S1), and a figure of the extended structure of **13** in crystal lattice showing the Cl1···H22C^a close contacts (Figure S2). This material is available free of charge via the Internet at http://pubs.acs.org.

References and Notes

(1) (a) Schmidpeter, A.; Bohm, R.; Groeger, H. *Angew. Chem., Int. Ed.* **1964**, *3*, 704. (b) Schmidpeter, A. and Stoll, K. *Angew. Chem., Int. Ed.* **1967**, *6*, 252. (c) Schmidpeter, A. and Stoll, A. *Angew. Chem., Int. Ed.* **1968**, *7*, 549.

(2) For reviews of early work, see (a) Silvestru, C.; Drake, J. E., *Coord. Chem. Rev*. **2001**, *223*, 117. (b) Ly, T. Q.; Woollins, J. D. *Coord. Chem. Rev.* **1998**, *176*, 451. (c) Haiduc, I.

in *Comprehensive Coordination Chemistry II*; McCleverty, J. A., Meyer, T. J. (Eds.); Elsevier Ltd; Amsterdam, 2003, p. 323-347.

(3) Rudler; H.; Denise, B.; Gregorio, J. R.; Vaissermann, J. *Chem. Commun*. **1997**, 229.

(4) Magennis, S. W.; Parsons, S.; Corval, A.; Woollins, J. D.; Pikramenou, Z. *Chem. Commun*. **1999**, 61.

(5) du Preez, J. G. H.; Knabl, K. U.; Krüger, L.; van Brecht, B. J. A. M. *Solvent Extr. Ion Exch*. **1992**, *10*, 729.

(6) For selected examples, see (a) Afzall, M.; Crouch, D.; Malik, M. A.; Motevalli, M.; O'Brien, P.; Park, J-H.; Woollins, J. D. *Eur. J. Inorg. Chem*. **2004**, 171. (b) Afzall, M.; Ellwood, K.; Pickett, N. L.; O'Brien, P.; Raftery, J.; Waters, J. *J. Mater. Chem*. **2004**, *14*, 1310. (c) Waters, J.; Crouch, D.; Raftery, J.; O'Brien, P. *Chem. Mater*. **2004**, *16*, 3289.

(7) Cupertino, D.; Birdsall, D. J.; Slawin, A. M. Z.; Woollins, J. D. *Inorg. Chim. Acta* **1999**, *290*, 1.

(8) Briand, G. G.; Chivers, T.; Parvez, M. *Angew. Chem., Int. Ed*. **2002**, *41*, 3468.

(9) Chivers, T.; Eisler, D. J.; Ritch, J. S.; Tuononen, H. M. *Angew. Chem., Int. Ed*. **2005**, *44*, 4953.

(10) Chivers, T.; Eisler, D. J.; Ritch, J. S. *Dalton Trans*., **2005**, 2675.

(11) Gaunt, A. J.; Scott, B. L.; Neu, M. P. *Angew. Chem., Int. Ed.*, **2006**, *45*, 1638.

(12) Garje, S.S.; Ritch, J. S.; Eisler, D. J.; Afzaal, M.; O'Brien, P.; Chivers, T. *J. Mater. Chem.*, **2006**, 966.

(13) Garje, S.S.; Eisler, D. J.; Ritch, J. S.; Afzaal, M.; O'Brien, P.; Chivers, T. *J. Am. Chem. Soc.*, **2006**, *128*, 3120

(14) Copsey, M. C.; Chivers, T. *Chem. Commun*., **2005**, 4938.

(15) The sulfur analog **2a** (R = ^{t}Bu derivative) and the selenium analogs **2b** (R = ^{i}Pr, ^{t}Bu derivatives) have been prepared in a similar manner and shown to have dimeric structures

with elongated E-E bonds: Chivers, T.; Eisler, D. J.; Ritch, J. S., manuscript in preparation.

(16) Konu, J.; Chivers, T; Tuononen, H. M. *Chem. Commun.* **2006**, 1634.

(17) Chivers, T. "*A Guide to Chalcogen-Nitrogen Chemistry"*, World Scientific, Singapore, **2005**, Chapter 4, pp. 60-63.

(18) Maaninen, A.; Chivers, T.; Parvez, M.; Pietikäinen, J.; Laitinen, R. S. *Inorg. Chem.* **1999**, *38*, 4093.

(19) Sheldrick, G. M. SHELXS-97, *Program for Crystal Structure Determination*, University of Göttingen, Germany, **1997**.

(20) Sheldrick, G. M. SHELXL-97, *Program for Crystal Structure Refinement*, University of Göttingen, Germany, **1997**.

(21) (a) Perdew, J. P.; Burke, K.; Ernzerhof, M. *Phys. Rev. Lett.* **1996**, *77*, 3865. (b) Perdew, J. P.; Burke, K.; Ernzerhof, M. *Phys. Rev. Lett***. 1997**, *78*, 1396. (c) Perdew, J. P.; Ernzerhof, M.; Burke, K. *J. Chem. Phys.* **1996**, *105*, 9982. (d) Ernzerhof, M.; Scuseria, G. E. *J. Chem. Phys.* **1999**, *110*, 5029.

(22) All basis sets were used as they are referenced in the Turbomole 5.8 internal basis set library. TURBOMOLE, Program Package for *ab initio* Electronic Structure Calculations, Version 5.8. R. Ahlrichs, *et al.* Theoretical Chemistry Group, University of Karlsruhe, Karlsruhe, Germany, 2005.

(23) Frisch, M. J.; Trucks, G. W.; Schlegel, H. B.; Scuseria, G. E.; Robb, M. A.; Cheeseman, J. R.; Montgomery, J. A.; Vreven, T.; Kudin, K. N.; Burant, J. C.; Millam, J. M.; Iyengar, S. S.; Tomasi, J.; Barone, V.; Mennucci, B.; Cossi, M.; Scalmani, G.; Rega, N.; Petersson, G. A.; Nakatsuji, H.; Hada, M.; Ehara, M.; Toyota, K.; Fukuda, R.; Hasegawa, J.; Ishida, M.; Nakajima, T.; Honda, Y.; Kitao, O.; Nakai, H.; Klene, M.; Li, X.; Knox, J. E.; Hratchian, H. P.; Cross, J. B.; Adamo, C.; Jaramillo, J.; Gomperts, R.; Stratmann, R. E.; Yazyev, O.; Austin, A. J.; Cammi, R.; Pomelli, C.; Ochterski, J. W.; Ayala, P. Y.;

Morokuma, K.; Voth, G. A.; Salvador, P.; Dannenberg, J. J.; Zakrzewski, V. G.; Dapprich, S.; Daniels, A. D.; Strain, M. C.; Farkas, O.; Malick, D. K.; Rabuck, A. D.; Raghavachari, K.; Foresman, J. B.; Ortiz, J. V.; Cui, Q.; Baboul, A. G.; Clifford, S.; Cioslowski, J.; Stefanov, B. B.; Liu, G.; Liashenko, A.; Piskorz, P.; Komaromi, I.; Martin, R. L.; Fox, D. J.; Keith, T.; Al-Laham, M. A.; Peng, C. Y.; Nanayakkara, A.; Challacombe, M.; Gill, P. M. W.; Johnson, B.; Chen, W.; Wong, M. W.; Gonzalez, C.; Pople, J. A. Gaussian 03, (Revision C.02), Gaussian, Inc., Pittsburgh, PA, 2003.

(24) This type of bonding interaction is well established in the solid-state structures of halide salts of certain cationic sulfur-nitrogen ring systems, *e.g.*, 1,2,3,4-dithiadiazolylium chlorides $[RCN_2S_2]Cl$ and $[S_4N_3]Cl$: (a) Rawson, J. R.; Banister, A. J.; Lavender, I. *Adv. Heterocyclic Chem*. **1995**, *62*, 137; (b) Galan-Mascaros, J-R.; Slawin, A. M. Z.; Woollins, J. D.; Williams, D. J. *Polyhedron*, **1996**, *15*, 4603.

(25) (a) Belluz, P. D. B.; Cordes, A. W.; Kristof, E. M.; Kristof, P. V.; Liblong, S. W.; Oakley, R. T. *J. Am. Chem. Soc*. **1989**, *111*, 9276; (b) Haas, A.; Kasprowski, J.; Pryka, M. *J. Chem. Soc., Chem. Commun*. **1992**, 1144.

(26) The Te-Te bond lengths of ditellurides are typically in the range 2.68-2.71 Å, but a value of 2.77 Å has been reported recently for the highly crowded system $(PhMe_2Si)_3CTe$-$TeC(SiMe_2Ph)_3$: Klapötke, T. M.; Krumm, B.; Nöth, H.; Gálvez-Ruiz, J. C.; Polborn, K.; Schwab, I.; Suter, M. *Inorg. Chem*. **2005**, *44*, 5254.

(27) Maaninen, T.; Tuononen, H. M.; Schatte, G.; Suontamo, R.; Valkonen, J.; Laitinen, R.; Chivers, T. *Inorg. Chem.* **2004**, *43*, 2097.

(28) The structures of the almost linear anion $[Te_3Ph_3]^-$ (Te-Te 2.939(1) and 3.112(1) Å) and the bent cation $[Te_3Ph_3]^+$ (Te-Te 2.979(1) and 3.049(1) Å) have been compared to that of I_3^-.[29]

(29) (a) Hillier, A. C.; Liu, S.-Y.; Sella, A.; Elsegood, M. R. J. *Angew. Chem Int. Ed*. **1999**, *38*, 2745 . (b) Jeske, J.; du Mont, W.; Jones, P. G. *Angew. Chem. Int. Ed.* **1997**, *36*, 2219.

(30) The bond orders were calculated by the Pauling equation $N = 10^{(D-R)/0.71}$,[31] where R is the observed bond length (Å). The single bond length D is estimated from the sums of appropriate covalent radii (Å):[31] Te-Te 2.74, Te-I 2.70, Te-Cl 2.36, Te-F 1.95, Se-Se 2.34, Se-I 2.50, Se-F 1.77.

(31) Pauling, L. *The Nature of the Chemical Bond*; 3rd Ed.; Cornell University Press; Ithaca, NY, **1960**.

(32) Maaninen, A.; Konu, J.; Laitinen, R. S.; Chivers, T.; Schatte, G.; Pietikäinen, J.; Ahlgrén, M. *Inorg. Chem.* **2001**, *40*, 3559.

(33) McWhinnie, W. R.; Thavornyutikarn, P. J. *Organomet. Chem.* **1972**, *35*, 149.

(34) Llabres, P. G.; Dideberg, O.; Dupont, L. *Acta Crystallogr.* **1972**, *B28*, 2438.

(35) The structure of an analogous six-membered ring system in the dimer $[N(PPh_2S)_2Te(\mu\text{-}Cl)]_2$ has been reported.[36]

(36) Novosad, J.; Törnroos, K. W.; Necas, M., Slawin, A. M. Z., Woollins, J. D.; Husebye, S. *Polyhedron* **1999**, *18*, 2861.

(37) Cea-Olivares, R.; Moya-Cabrera, M.; Garcia-Montalvo, V.; Castro-Blanco, R.; Toscano, R. A.; Hernandez-Ortega, S. *Dalton Trans.* **2005**, 1017.

(38) The structure of **12,** obtained as a hydrolysis product of $K[N(PPh_2Se)_2]$, has been mentioned briefly in a review,[39] but details of the crystallographic and structural data have not been reported.

(39) Woollins, J. D. *J. Chem. Soc., Dalton Trans.* **1996**, 2893.

(40) Slawin, A. M. Z; Smith, M. B.; Woollins, J. D. *Chem. Commun.* **1996**, 2095.

(41) Briand, G.G.; Chivers, T.; Krahn, M.; Parvez, M. *Inorg. Chem*. **2002**, *41*, 6808, and references cited therein.

(42) The hydrolysis product $\{[N(PPh_2)_2Se]_2(\mu\text{-}O)\}$ (**12**) is also expected to give rise to two resonances with a relative intensity of 1:1, one of which would show a $^1J(^{77}Se,^{31}P)$ coupling constant in the region 720-750 Hz for the terminal P=Se bond. It is highly

unlikely, however, that the solvent used in several different reactions would contain the exact amount of water to give a 2:1 mixture of **10** and the hydrolysis product **12** that is required to generate three resonances with a 2:1:1 intensity ratio in the ^{31}P NMR spectrum (see Scheme 1).[43]

(43) The reaction between [(TMEDA)NaN($PPh_2Se)_2$] and I_2 was also conducted in n-hexane/toluene solution and gave a 1:1 mixture of **10** and **11** (^{31}P NMR spectrum), thus precluding the unlikely possibility that THF is the source of oxygen in the formation of **12**.

(44) The syntheses of the following related acyclic compounds $EP(R_2)NP(R_2)X$ (E = chalcogen; X = halogen) have been reported without structural characterization: [$SP(Ph_2)N(Ph_2)PCl$],[45a] [$SP(Ph_2)N(Ph_2)PCl$]HCl,[45a] [$SP(Ph_2)N(Ph_2)PBr$],[45b] [$OP(Ph_2)N(Ph_2)PCl$],[45c] and [$OP(Ph_2)N(Ph_2)PBr$]Br.[45d]

(45) (a) Schmidpeter, A.; Groeger, H. *Chem. Ber.* **1967**, *100*, 3979. (b) Meinel, L.; Nöth, H. *Z. Anorg. Allg. Chem.* **1970**, *373*, 36. (c) Gilson, I. T.; Sisler, H. H. *Inorg. Chem.* **1965**, *4*, 273. (d) Baldwin, R. A.; Washburn, R. M. *J. Org. Chem.* **1965**, *30*, 2093.

Table 1. Crystallographic data for $[N(P^iPr_2Se)_2]SbF_6$ (**6**), $[N(P^iPr_2Te)_2]SbF_6$ (**7**), $[N(P^iPr_2Te)_2]Cl$ (**8**), $[N(PPh_2Te)_2]I$ (**9**), $[N(PPh_2Se)_2(\mu\text{-}Se)][I]$ (**10**), $\{[N(PPh_2)_2Se]_2(\mu\text{-}O)\}\bullet CH_2Cl_2$ (**12**$\bullet CH_2Cl_2$) and $[SeP(^iPr_2)N(^iPr_2)PCl]$ (**13**).[a]

	6	**7**	**8**	**9**	**10**	**12**	**13**
empirical formula	$C_{12}H_{28}F_6N$ P_2SbSe_2	$C_{12}H_{28}F_6N$ P_2SbTe_2	$C_{12}H_{28}ClN$ P_2Te_2	$C_{24}H_{20}IN$ P_2Te_2	$C_{24}H_{20}IN$ P_2Se_3	$C_{49}H_{42}Cl_2N_2O$ P_4Se_2	$C_{12}H_{28}ClN$ P_2Se
fw	641.96	739.24	538.94	766.45	748.13	1027.55	362.70
crystal system	triclinic	monoclinic	monoclinic	triclinic	monoclinic	monoclinic	orthorhombic
space group	*P*-1	$P2_1/n$	$P2_1/c$	*P*-1	$P2_1/c$	$C2/c$	$P2_12_12_1$
a, Å	8.877(2)	9.996(2)	7.398(2)	10.592(2)	9.424(2)	10.765(2)	7.038(1)
b, Å	10.205(2)	8.960(2)	17.778(4)	11.125(2)	20.694(4)	20.093(4)	13.483(3)
c, Å	13.078(3)	25.778(5)	14.918(3)	12.264(3)	13.016(3)	21.546(4)	18.421(4)
α, deg.	68.38(3)	90.00	90.00	95.51(3)	90.00	90.00	90.00
β, deg.	79.18(3)	90.24(3)	103.27(3)	100.35(3)	95.07(3)	92.34(3)	90.00
γ, deg.	88.16(3)	90.00	90.00	117.98(3)	90.00	90.00	90.00
V, $Å^3$	1080.9(5)	2308.7(8)	1909.6(7)	1228.1(6)	2528.6(9)	4657(2)	1748.0(6)
Z	2	4	4	2	4	4	4
T, °C	-100	-100	-100	-100	-100	-100	-100
ρ_{calcd}, g/cm^3	1.972	2.127	1.875	2.073	1.965	1.466	1.378
μ(Mo Kα), mm^{-1}	4.837	3.854	3.350	3.774	5.725	1.879	2.468
crystal size, mm^3	0.28x0.24x0.24	0.16x0.16x0.08	0.36x0.16x0.16	0.08x0.04x0.03	0.12x0.04x0.01	0.12x0.08x0.08	0.16x0.16x0.16

$F(000)$	620	1384	1032	716	1424	2080	752
Θ range, deg	3.71-25.03	3.15-25.03	3.62-25.03	2.25-25.02	2.75-25.01	2.38-25.03	3.22-25.01
reflns collected	7037	7775	12523	8369	8122	6107	6482
unique reflns	3803	4062	3352	4326	4447	4102	3049
R_{int}	0.0161	0.0417	0.0501	0.0318	0.0379	0.0275	0.0552
reflns [$I>2\sigma(I)$]	3463	3028	2805	3651	3403	3300	2634
R_1 [$I>2\sigma(I)$] [b]	0.0210	0.0345	0.0321	0.0265	0.0465	0.0376	0.0400
wR_2 (all data) [c]	0.0475	0.0725	0.0703	0.0583	0.1105	0.0850	0.0905
GOF on F^2	1.045	1.021	1.085	1.041	1.106	1.023	1.034
completeness	0.995	0.995	0.996	0.997	0.995	0.996	0.991

[a] λ (MoKα) = 0.71073 Å. [b] $R_1 = \Sigma \big| |F_o| - |F_c| \big| / \Sigma |F_o|$. [c] $wR_2 = [\Sigma w(F_o^2-F_c^2)^2/\Sigma wF_o^4]^{½}$.

Table 2. Selected bond lengths (Å) and bond angles (°) in **4**-**9** [calculated bond orders in square brackets[30]].

	4[16]	**5**[16]	**6**	**7**	**8**	**9**
E1-E2	2.484(1) [0.63]	2.840(1) [0.72]	2.348(1) [0.97]	2.7162(7) [1.08]	2.9026(7) [0.59]	2.846(1) [0.71]
E1-P1	2.273(2)	2.396(3)	2.273(1)	2.497(2)	2.500(1)	2.510(1)
E2-P2	2.229(2)	2.437(3)	2.2628(9)	2.485(2)	2.443(1)	2.457(1)
P1-N1	1.593(5)	1.621(6)	1.595(2)	1.588(5)	1.592(4)	1.586(4)
P2-N1	1.590(5)	1.552(6)	1.591(2)	1.596(4)	1.596(4)	1.601(3)
E1···X1	3.150(1) [0.12]	3.430(1) [0.09]	2.981(3) [0.02]	3.120(4)	2.687(2) [0.35]	3.169(1) [0.22]
E1···E1’			3.868(2)[b] [0.04]			3.917(2)[e] [0.02]
E1···E2’			3.911(1)[b] [0.006]	4.0302(8)[c] [0.02]	4.3112(8)[d] [0.006]	
E2···X1’	4.006(1)[a] [0.008]	3.494(1)[a] [0.08]				3.737(1)[e] [0.03]
E2···X2’			3.329(2)[b] [0.006]			
E2···E2’					3.584(1) [0.06]	
P1-N1-P2	128.3(4)	133.2(4)	126.1(1)	130.6(3)	131.7(3)	130.3(2)
N1-P1-E1	108.4(2)	109.6(2)	106.73(9)	108.1(2)	111.2(2)	111.4(1)
N1-P2-E2	108.7(2)	109.4(2)	107.94(8)	109.5(2)	110.5(2)	112.4(1)
P1-E1-E2	91.41(4)	88.56(5)	92.60(3)	88.57(4)	86.56(3)	87.73(4)
P2-E2-E1	93.94(4)	88.36(5)	93.81(3)	89.38(4)	88.53(3)	89.95(4)
P1-E1-E2-P2	25.05(7)	25.84(7)	29.10(3)	28.15(5)	25.88(4)	21.16(3)

Symmetry operations: [a] x, y-1, z; [b] 2-x, 1-y, 1-z; [c] 1-x, 1-y, -z; [d] 1-x, 1-y, 1-z; [e] 1-x, 2-y, 1-z.

Table 3. Selected bond lengths (Å) and bond angles (°) in **10**, **12**•CH_2Cl_2 and **13**.

		10	
Se1-Se3	2.441(1)	P1-N1	1.588(6)
Se2-Se3	2.427(1)	P2-N1	1.591(6)
Se1-P1	2.222(2)	Se3···I1	3.102(1)
Se2-P2	2.202(2)	Se3···I1'	3.140(1)[a]
P1-N1-P2	131.7(4)	P1-Se1-Se2	98.14(6)
N1-P1-Se1	115.7(2)	P2-Se2-Se1	96.38(6)
N1-P2-Se2	116.0(2)	Se1-Se2-Se3	95.64(4)
		12•CH_2Cl_2	
Se1-P1	2.117(1)	P2-N1	1.549(3)
P1-N1	1.620(3)	O1-P2	1.619(1)
Se1-P1-N1	118.4(1)	P2-O1-P2'	139.8(2)[b]
P1-N1-P2	135.6(2)	P1-N1-P2-O1	63.3(3)
N1-P2-O1	115.3(1)	P2-N1-P1-Se1	8.7(3)
		13	
Se1-P1	2.125(1)	P1-N1	1.626(3)
Cl1-P2	2.050(2)	P2-N1	1.532(3)
Se1-P1-N1	118.1(1)	P1-N1-P2-Cl1	43.5(5)
P1-N1-P2	147.0(2)	P2-N1-P1-Se1	8.3(6)
N1-P2-Cl1	114.9(1)		

Symmetry operations: [a] 1-x, 1-y, -z; [b] 1-x, y, 1.5-z.

Figure Captions

Figure 1. Molecular structures of (a) $[N(P^iPr_2Se)_2]I$ (**4**) and $[N(P^iPr_2Te)_2]I$ (**5**),[16] (b) $[N(P^iPr_2Se)_2]SbF_6$ (**6**), (c) $[N(P^iPr_2Te)_2]SbF_6$ (**7**) and (d) $[N(P^iPr_2Te)_2]Cl$ (**8**) with the atomic numbering scheme. Hydrogen atoms have been omitted for clarity. Symmetry operation: [a] x, y-1, z; [b] 2-x, 1-y, 1-z; [c] 1-x, 1-y, -z; [d] 1-x, 1-y, 1-z.

Figure 2. Crystal packing in (a) **6** and (b) **7** viewed along a-axis. Hydrogen atoms have been omitted for clarity.

Figure 3. Frontier molecular orbitals and energy levels in the $[N(P^iPr_2E)_2]^+$ rings (E = Se, Te).

Figure 4. Molecular structures of (a) $[N(PPh_2Te)_2]I$ (**9**), (b) $[N(PPh_2Se)_2(\mu\text{-}Se)][I]$ (**10**) and (c) $\{[N(PPh_2)_2Se]_2(\mu\text{-}O)\}\bullet CH_2Cl_2$ (**12**•CH_2Cl_2) with the atomic numbering scheme. Hydrogen atoms and the solvent molecule in the structure **12**•CH_2Cl_2 have been omitted for clarity. Symmetry operation: [a] 1-x, 2-y, 1-z; [b] 1-x, 1-y, -z; [c] 1-x, y, 1.5-z.

Figure 5. Crystal packing in **10** showing the planar arrangement of the phenyl groups.

Figure 6. Molecular structure of $[SeP(^iPr_2)N(^iPr_2)PCl]$ (**13**). Hydrogen atoms have been omitted for clarity.

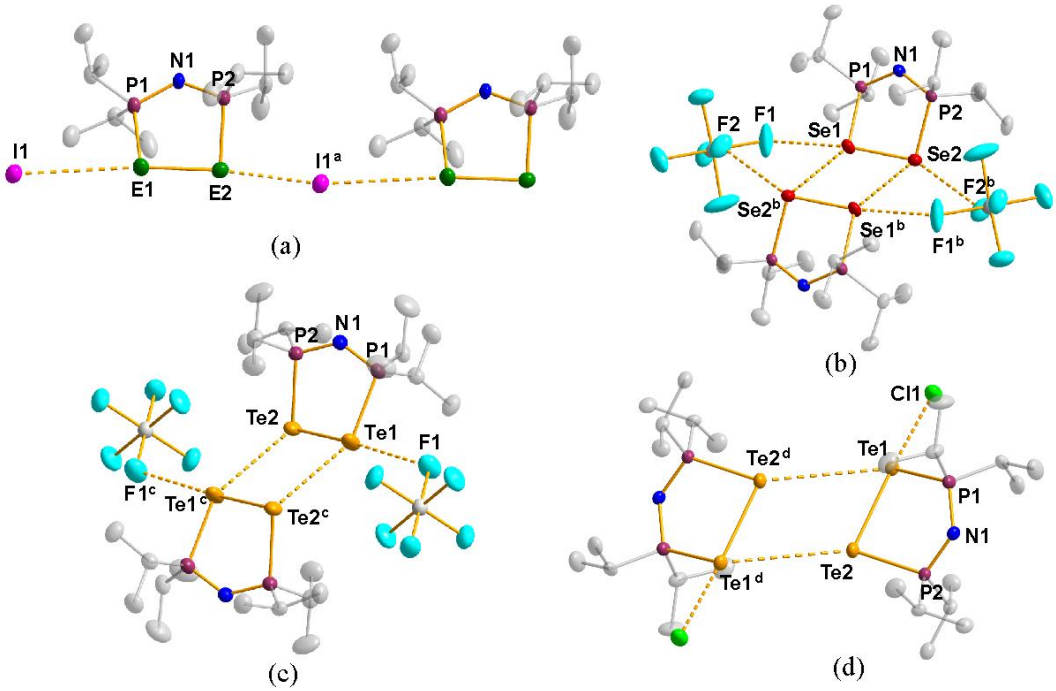
I1
N1
P1
P2
E1
E2
I1a
(a)
F2
F1
Se1
N1
P1
P2
Se2
F2b
Se2b
Se1b
F1b
(b)
P2
N1
P1
Te2
Te1
F1
F1c
Te1c
Te2c
(c)
Cl1
Te2d
Te1
P1
N1
Te1d
Te2
P2
(d)

Figure 1.

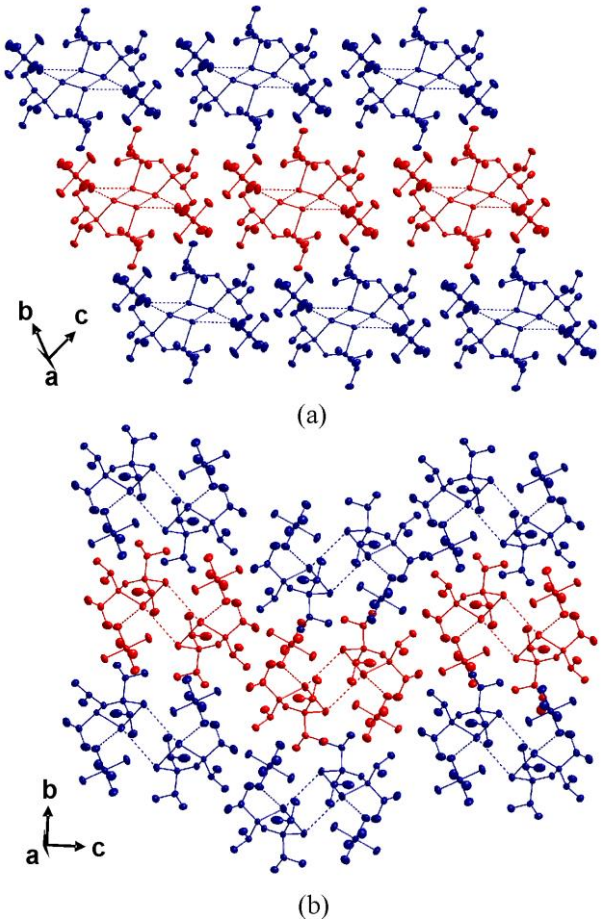

Figure 2.

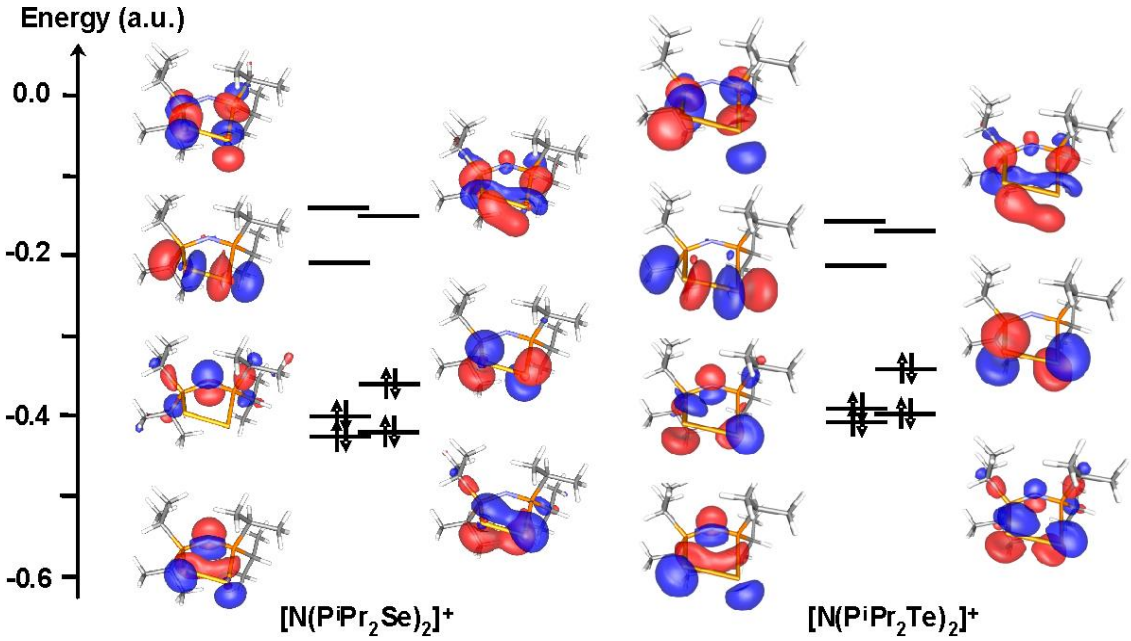

Figure 3.

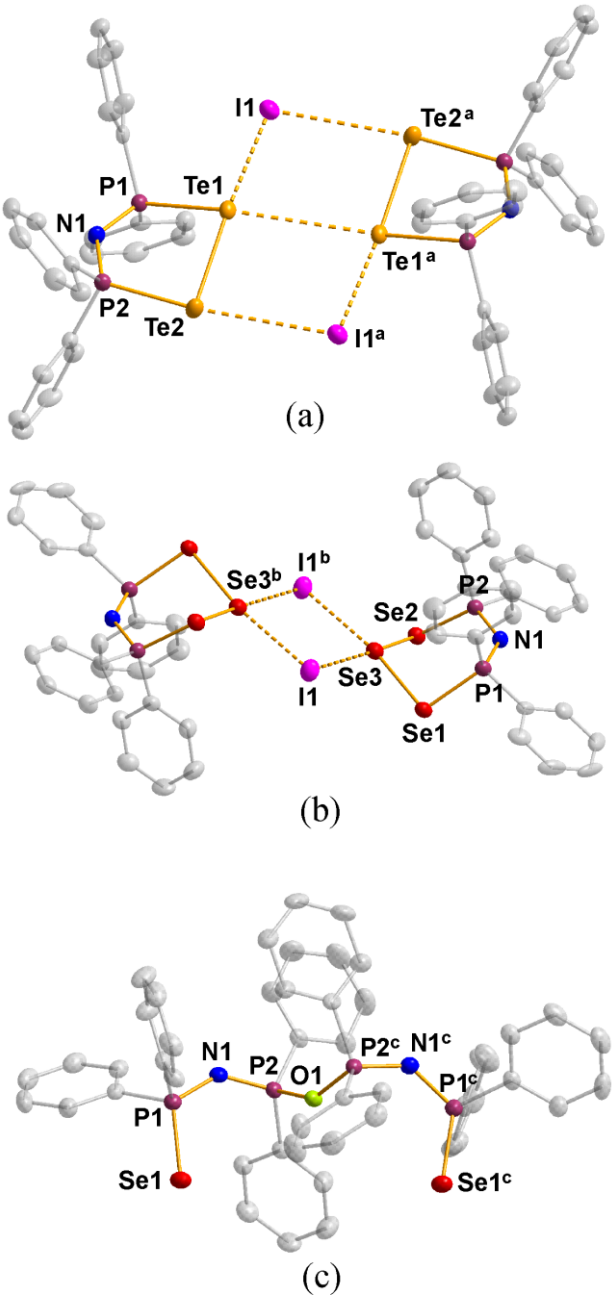
I1
Te2a
P1
Te1
N1
Te1a
P2
Te2
I1a
(a)
Se3b
I1b
P2
Se2
N1
Se3
I1
P1
Se1
(b)
N1
P2
O1
P2c
N1c
P1c
P1
Se1
Se1c
(c)

Figure 4.

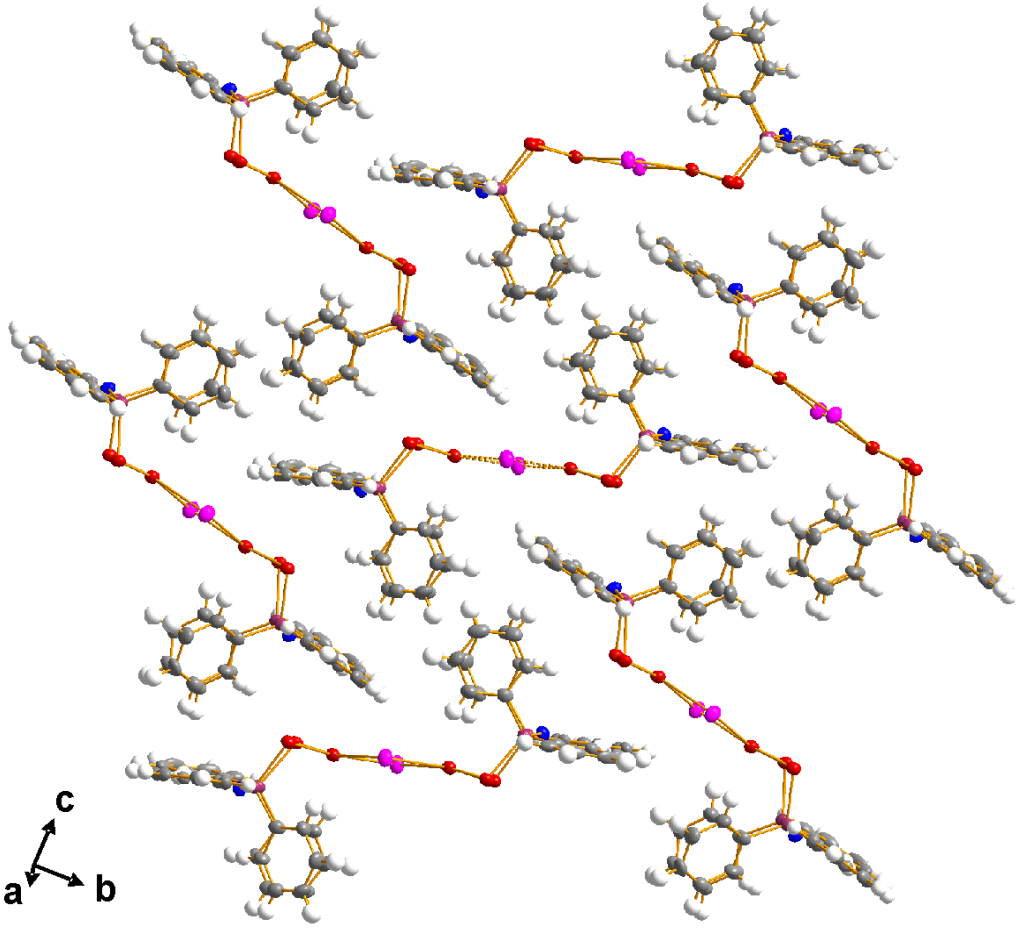

Figure 5.

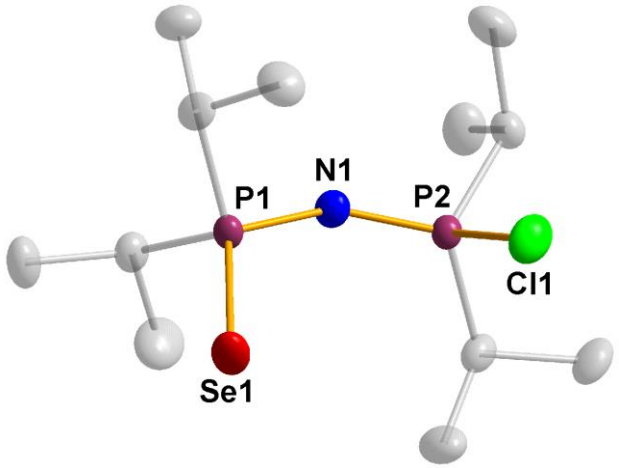

Figure 6.